

# **Propensity of heavier halides for the water/vapor interface revisited using the Amoeba force field**

**Lukáš Tůma, Dominik Jeníček, and Pavel Jungwirth\***

*Institute of Organic Chemistry and Biochemistry, Academy of Sciences of the Czech Republic  
and Center for Biomolecules and Complex Molecular Systems, Flemingovo nám. 2, 16610  
Prague 6, Czech Republic*

\*Corresponding author. E-mail: pavel.jungwirth@uochb.cas.cz, FAX: +420-220 410 320

## **Abstract**

Molecular dynamics simulations of aqueous sodium halide solutions in slab geometry were performed using the state-of-the-art polarizable Amoeba force field. The present calculations reveal a propensity of halide anions for the water/vapor interface, which correlates with the ionic size and polarizability and, therefore, increases in the series  $\text{Cl}^- < \text{Br}^- < \text{I}^-$ . These results are in a quantitative agreement with previous calculations employing much simpler polarizable potentials and are supported by a mounting experimental evidence from photoelectron and non-linear optical and vibrational spectroscopies.

## I. INTRODUCTION

The propensity of chloride, bromide, and iodide for the water/vapor interface (or, for finite salt concentrations more precisely aqueous solution/vapor interface) has been predicted by recent molecular dynamics simulations of extended aqueous slabs employing polarizable potentials [1-3]. This result is in contradiction with the traditional model of surfaces of electrolytes within which atomic ions are repelled from the water/vapor interface by electrostatic image forces [4-5]. It has been argued recently that other forces, such as polarization interactions and specific interactions within the first solvation shell can in some cases drive simple inorganic ions to the surface [2-3,6-7]. Similar behavior was observed in water clusters where asymmetric (surface) solvation of heavier halides was both seen in *ab initio* and molecular dynamics calculations and confirmed by photoelectron spectroscopy already in the 1990s [8-10]. Finite size clusters, however, differ in many aspects from extended systems and it was suggested that it is the curvature effect that primarily drives ions such as chloride to the cluster surface [11]. Until several years ago, no direct experimental evidence concerning the presence of simple inorganic ions at the extended water/vapor interface was available. Most recently, the situation has changed thanks to spectroscopic techniques, such as the non-linear vibrational sum frequency generation (VSFG) [12-13] and second harmonic generation (SHG) [14-15] spectroscopies, and high-pressure photoelectron spectroscopy (PES) [16-17], which in most cases confirm the presence and even accumulation of polarizable (soft) anions, such as iodide, bromide, azide, thiocyanate, etc., at the water/vapor interface.

Since meaningful molecular dynamics (MD) simulations of ions at the water/vapor interface require systems with hundreds to thousands of atoms in the unit cell and simulation times in the 100 ps to nanosecond scale, computational feasibility dictates the use of a relatively simple force field. Indeed, even the most extensive first principle (*ab initio*) MD simulations are only slowly starting to approach these system size and time scale requirements [18]. Therefore, we remain to be dependent on empirical potentials, albeit carefully parametrized against accurate

experiments and ab initio calculations for small model systems. In our previous studies of ions in aqueous slabs [1,3] we have used a relatively simple force field employing a three-site rigid water model (POL3) [19] and isotropic atomic polarizabilities on all ions and water oxygens. Other researchers employed a slightly more sophisticated four-site polarizable water potential (DC97) [20], reaching essentially the same conclusions [2].

In the meanwhile, several new polarizable water models have been developed. These potentials combine a more complex functional form with careful fitting to a large set of experimental and theoretical data. Typical representatives of these “new generation” water potentials are the TTM2 [21], POL5/QZ [22], SAPT [23], VRT(ASP-W) [24], and the Amoeba [25] models. We ask ourselves the question how will our results concerning the propensity of heavier halides for the water/vapor interface stand in the light of these new potentials. The last one is particularly suitable for our purpose since it also contains a consistent parametrization of alkali cations and halide anions [26]. Therefore, in this study we tested our theoretical predictions by performing slab simulations of aqueous sodium chloride, bromide, and iodide using the Amoeba force field. In addition to previous benchmarking against first principle calculations on small cluster models [3,10,27] the present results add to the robustness of our fundamental conclusion that heavier halides can be found at the water/vapor interface and bromide and iodide even exhibit surfactant activity, i.e., their concentration at certain regions of the interface is higher than that in the bulk. Such conclusion not only has an important methodological impact but also has direct implications, e.g., for heterogeneous tropospheric chemistry on aqueous sea salt aerosols [28].

## II. SYSTEMS AND COMPUTATIONAL METHODS

Molecular dynamics simulation were performed for extended aqueous systems in a slab geometry containing 214 water molecules, 4 sodium cations, and 4 halide (chloride, bromide, or iodide) anions in a 18.6 x 18.6 x 50 Å prismatic unit cell, corresponding roughly to a 1 M salt

concentration. The extension of one of the box dimensions leads to the slab arrangement of the system with two water/vapor interfaces [29-30]. Due to large computational requirements of calculations with the Amoeba potential the present system size is smaller than than employed previously with simpler polarizable force fields [1-3]. However, as shown recently [18], it is large enough to support a stable aqueous slab. For the calculations with periodic boundaries the non-bonded interactions were cut off at 9 Å. Long range monopolar electrostatic interactions were accounted for using the particle mesh Ewald procedure [31], while a conventional Ewald summation [32] was used for summing the multipolar terms. A polarizable Amoeba force field was employed both for water and the ions [25-26]. Within this force field, each atomic site possesses for intermolecular interactions a permanent charge, dipole, and quadrupole, as well as a 14-7 van der Waals term, and scalar polarizability.

All these simulations were performed in the NVT ensemble at 300 K. Systems were first equilibrated for at least 200 ps with a subsequent 500 ps production run. The timestep was set to 1 fs and all OH bonds were constrained using the RATTLE algorithm [33]. In addition, geometry minimizations were performed for clusters containing 1-6 water molecules and a single halide anion. All calculations were performed using Tinker version 3.9 [34].

### III. RESULTS AND DISCUSSION

Before running extended slab simulations, we performed benchmarking structure minimizations for clusters containing a single heavier halide anion (chloride, bromide, or iodide) and 1-6 water molecules. Previous ab initio calculations and molecular dynamics simulations, supported by photoelectron and vibrational spectroscopy measurements, showed that up to four waters are in direct contact with the anion, while the subsequent water molecules start to build up a second solvation shell of an asymmetrically solvated ion [8-10]. The present results with the Amoeba potential, as well as recent benchmark Amoeba calculations of sequential hydration of

$\text{Cl}^-$  [26], are in perfect agreement with this picture. This is demonstrated in Fig. 1 which depicts optimized geometries of the (largest investigated) heavier halide – water hexamer clusters. In all three cases, four water molecules are directly bound to the halide anion, while the remaining two waters participate only in water-water hydrogen bonding. The structures for clusters containing chloride, bromide, or iodide are very similar to each other, except that the ion-water distances increase upon moving down the periodic table (see Fig. 1). The total binding energies of the clusters also decreases in this order, being 88.2 kcal/mol for  $\text{Cl}^-(\text{H}_2\text{O})_6$ , 81.6 kcal/mol for  $\text{Br}^-(\text{H}_2\text{O})_6$ , and 75.2 kcal/mol for  $\text{I}^-(\text{H}_2\text{O})_6$ .

Molecular dynamics simulations of salt solutions in slab geometries were used to extract density profiles, i.e., the distributions of ions from the aqueous bulk to the the water/vapor interface. The most interesting issue is the comparison of the ionic density profiles to that of water itself, particularly in the interfacial region. If the ion signal monotonically decays before that of water, one has a case of ion repulsion from the interface in accord with the standard electrostatic model [4-5]. If however, the ion signal pertains all the way to the interface or even exhibits a surface peak we can talk about a “non-classical” behavior. Of course, the density profiles of the cationic and anionic component of a given salt can have very different shapes in the interfacial region.

The density profiles for 1 M aqueous NaCl are shown in Fig. 1. Since the two halves of the slab are, in principle, equivalent, we averaged the curves over them and show the data as a function of the z-coordinate spanning the bulk liquid and the vapor region across the water/vapor interface. We see that, in accord with the standard picture, the signal from the small non-polarizable sodium cations decreases to zero about 3 Å (i.e., roughly one water layer) before water density does. However, the larger and more polarizable chloride anions penetrate all the way the the surface and their density profile closely follows that of water. These results are in quantitative agreement with previous simulations employing a significantly simpler polarizable force field [1].

The density profiles of dissolved NaBr are even more interesting, since large and soft bromide anions actually exhibit surface enhancement, followed by subsurface depletion. Sodium cations, which are strongly repelled from the surface, nevertheless tend to accumulate in the subsurface due to the electrostatic attraction from the surface adsorbed bromide anions. This factor of two maximal surface enhancement of bromide is again in excellent agreement with previous results [1]. The subsurface behavior is also similar, although the effect of the smaller size of the present system also comes into play here.

Iodide is the largest and softest among the investigated ions and it also exhibits the strongest surface propensity. Again in quantitative agreement with previous simulations [1] there is a roughly 2.5-fold peak surface enhancement, followed by subsurface depletion in a region, where the sodium density is enhanced. Thus, for all the three sodium halide solutions the Amoeba force field yields predictions for the surface propensity of heavier halides, which are in quantitative agreement with results obtained with the simple POL3 model of water and polarizable ions.

#### **IV. CONCLUSIONS**

Molecular dynamics simulations employing the recently developed polarizable Amoeba force field reveal an increasing propensity of heavier halides ( $\text{Cl}^- < \text{Br}^- < \text{I}^-$ ) for the surfaces of aqueous sodium halide solutions. The amount of anionic surface enhancement, accompanied with subsurface depletion, correlates with the ionic size and polarizability and quantitatively agrees with previous results obtained using much less sophisticated polarizable potentials [1]. This fact, in addition to mounting experimental evidence, provides support to the emerging picture of surfaces of electrolytes [Jungwirth05], where ion specificity plays a crucial role and certain ions (such as the heavier halides) are present and can even be enhanced at the surface.

## **Acknowledgements**

We thank Greg Voth and Doug Tobias for fruitful discussions. Support from the Czech Ministry of Education (grant LC512) and from the US-NSF (grants CHE 0431512 and 0209719) is gratefully acknowledged.

## References:

1. P. Jungwirth and D. J. Tobias, *J. Phys. Chem. B* 105 (2001) 10468.
2. L. X. Dang and T. M. Chang, *J. Phys. Chem. B* 106 (2002) 235.
3. P. Jungwirth and D. J. Tobias, *J. Phys. Chem. B* 106 (2002) 6361.
4. L. Onsager and N. N. T. Samaras, *J. Chem. Phys.* 2 (1934) 528.
5. J. E. B. Randles, *Phys. Chem. Liq.* 7 (1977) 107.
6. L. Frediani, B. Mennucci, and R. Cammi, *J. Phys. Chem. B* 108 (2004) 13796.
7. D. H. Herce, L. Perera, T. A. Darden, and C. Sagui, *J. Chem. Phys.* 122 (2005) 024513.
8. L. Perera and M. L. Berkowitz, *J. Chem. Phys.* 95 (1991) 1954.
9. G. Markovich, G. Pollack, R. Giniger, and O. Cheshnovsky, *J. Chem. Phys.* 101 (1994) 9344.
10. R. W. Gora, S. Roszak, and J. Leszczynski, *Chem. Phys. Lett.* 325 (2000) 7.
11. S. J. Stuart and B. J. Berne, *J. Phys. Chem. A* 103 (1999) 10300.
12. D. F. Liu, G. Ma, L. M. Levering, and H. C. Allen, *J. Phys. Chem. B* 108 (2004) 2252.
13. E. A. Raymond and G. L. Richmond, *J. Phys. Chem. B* 108 (2004) 5051.
14. P. B. Petersen, J. C. Johnson, K. P. Knutsen, and R. J. Saykally, *Chem. Phys. Lett.* 397 (2004) 46.
15. P. B. Petersen and R. J. Saykally, *Chem. Phys. Lett.* 397 (2004) 51.
16. S. Ghosal, J. C. Hemminger, H. Bluhm, B. S. Mun, E. L. D. Hebenstreit, G. Ketteler, D. F. Ogletree, F. X. Requejo, and M. Salmeron, *Science* 307 (2005) 563.
17. R. Weber, B. Winter, P. M. Schmidt, W. Widdra, I. V. Hertel, M. Dittmar, and M. Faubel, *J. Phys. Chem. B* 108 (2004) 4729.
18. I. F. W. Kou and C. J. Mundy, *Science* 303 (2004) 658.
19. J. W. Caldwell and P. A. Kollman, *J. Phys. Chem.* 99 (1995) 6208.

20. L. X. Dang and T.-M. Chang, *J. Chem. Phys.* 106 (1997) 8149.
21. C. J. Burnham and S. S. Xantheas, *J. Chem. Phys.* 116 (2002) 5115.
22. H. A. Stern, F. Rittner, B. J. Berne, and R. A. Friesner, *J. Chem. Phys.* 115 (2001) 2237.
23. E. M. Mas, R. Bukowski, and K. Szalewicz, *J. Chem. Phys.* 118 (2003) 4386.
24. N. Goldman and R. J. Saykally, *J. Chem. Phys.* 120 (2004) 4777.
25. P. Ren and J. W. Ponder, *J. Phys. Chem. B* 107 (2003) 5933.
26. A. Grossfield, P. Ren, and J. W. Ponder, *J. Am. Chem. Soc.* 125 (2003) 15671.
27. D. J. Tobias, P. Jungwirth, and M. Parrinello, *J. Chem. Phys.* 114 (2001) 7036.
28. E. M. Knipping, M. J. Lakin, K. L. Foster, P. Jungwirth, D. J. Tobias, R. B. Gerber, D. Dabdub, and B. J. Finlayson-Pitts, *Science* 288 (2000) 301.
29. M. A. Wilson and A. Pohorille, *J. Chem. Phys.* 95 (1991) 6005.
30. I. Benjamin, *J. Chem. Phys.* 95 (1991) 3698.
31. U. Essmann, L. Perera, M. L. Berkowitz, T. Darden, H. Lee, and L. G. Pedersen, *J. Chem. Phys.* 103 (1995) 8577.
32. J. W. Perram, H. G. Petersen, and S. W. De Leeuw, *Mol. Phys.* 65 (1988) 875.
33. H. C. Andersen, *J. Comput. Phys.* 52 (1983) 24.
34. J. W. Ponder, TINKER: Software tools for molecular design. Version 3.9, Saint Louis, MO, 2001.
35. [Jungwirth05] M. Mucha, T. Frigato, L. M. Levering, H. Allen, D. J. Tobias, L. X. Dang, and P. Jungwirth, *J. Phys. Chem. B* 109 (2005) 7617.

## Figure Captions

**Figure 1:** Structures of the  $X^-(\text{H}_2\text{O})_6$  clusters. A)  $X = \text{Cl}$ , B)  $X = \text{Br}$ , and C)  $X = \text{I}$ .

**Figure 2:** Density profiles (i.e., histogrammed densities of the electrolyte ions and water molecules in layers parallel to the surface, from the center of the slab across the interface into the gas phase) for 1 M aqueous NaCl.

**Figure 3:** Density profiles of individual species for 1 M NaBr in an aqueous slab.

**Figure 4:** profiles of individual species for 1 M NaI in an aqueous slab.

**Figure 1:**

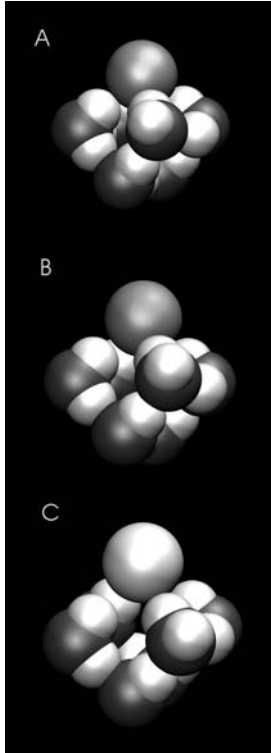


**Figure 2:**

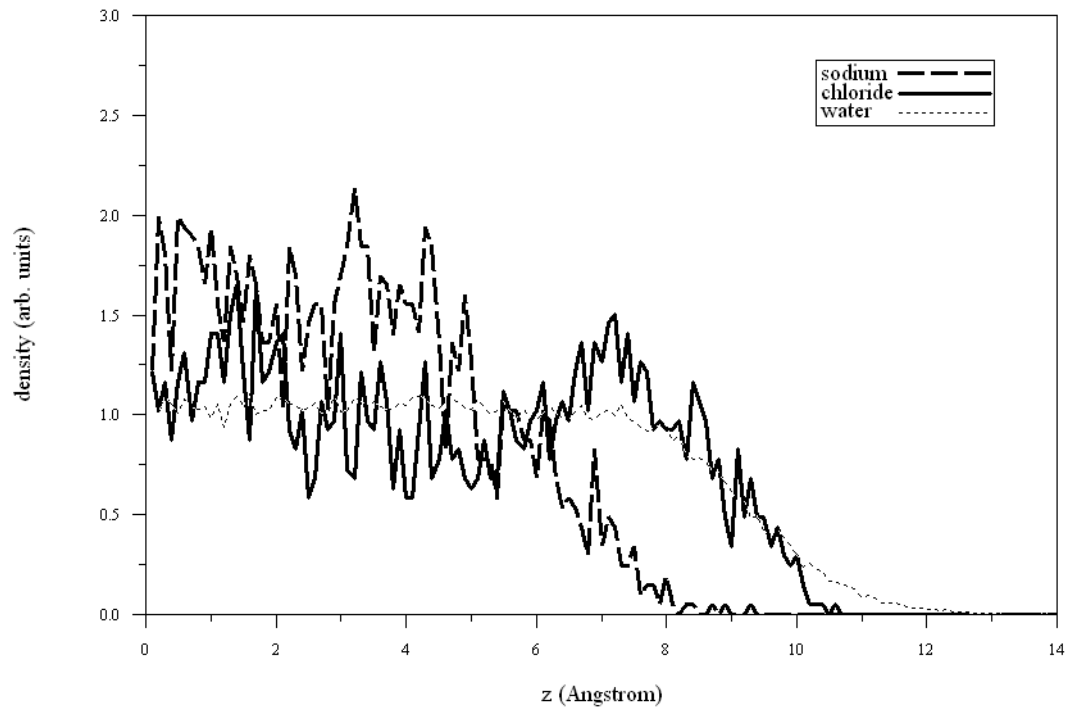


**Figure 3:**

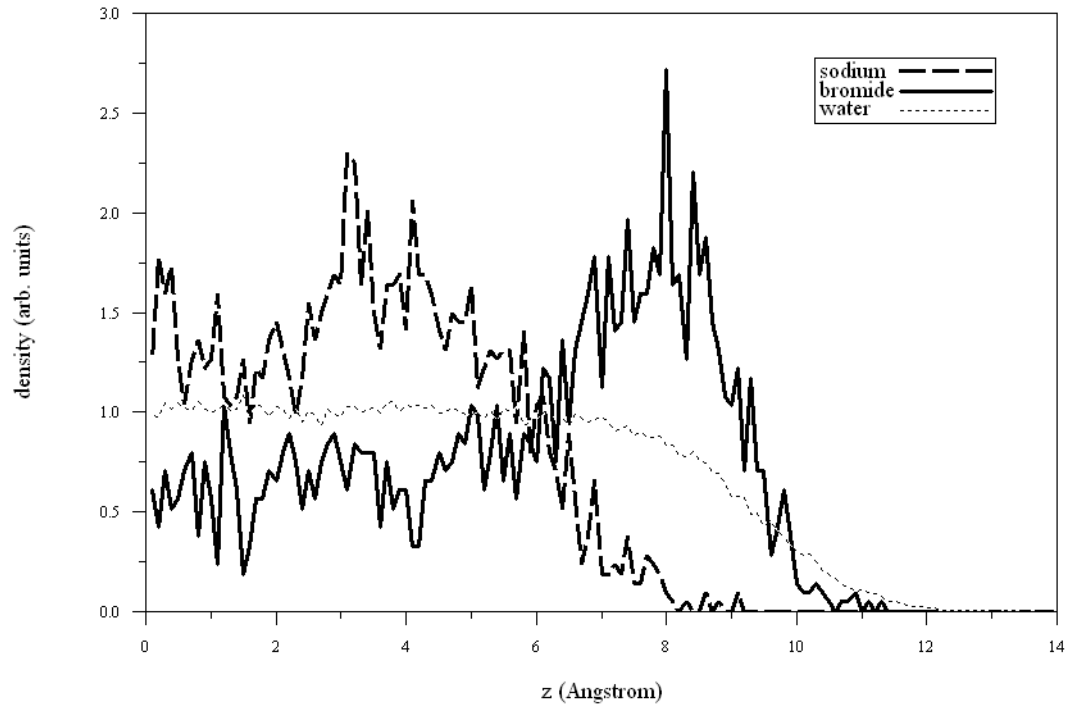


Figure 4:

